

Magnetic field resistant quantum interferences in bismuth nanowires based Josephson junctions

Chuan Li¹, A. Kasumov^{1,5}, A. Murani¹, Shamashis Sengupta², F. Fortuna², K. Napolskii^{3,4}, D. Koshkodaev⁴, G. Tsirlina³, Y. Kasumov⁵, I. Khodos⁵, R. Deblock¹, M. Ferrier¹, S. Guéron¹ and H. Bouchiat¹

¹ *LPS, Univ. Paris-Sud, CNRS, UMR 8502, F-91405 Orsay Cedex, France*
² *CSNSM, Univ. Paris-Sud, IN2P3, UMR 8609, F-91405 Orsay Cedex, France*

³ *Faculty of Chemistry, Moscow State University, Leninskie Gory, 1-blg.3, Moscow, 119991, Russia*

⁴ *Department of Material Sciences, Moscow State University, Leninskie Gory, Moscow, 119991, Russia and*

⁵ *Institute of Microelectronics Technology and High Purity Materials, RAS, ac. Ossipyan, 6, Chernogolovka, Moscow Region, 142432, Russia*

We investigate proximity induced superconductivity in micrometer-long bismuth nanowires connected to superconducting electrodes with a high critical field. At low temperature we measure a supercurrent that persists in magnetic fields as high as the critical field of the electrodes (above 11 T). The critical current is also strongly modulated by the magnetic field. In certain samples we find regular, rapid SQUID-like periodic oscillations occurring up to high fields. Other samples exhibit less periodic but full modulations of the critical current on Tesla field scales, with field-caused extinctions of the supercurrent. These findings indicate the existence of low dimensionally, phase coherent, interfering conducting regions through the samples, with a subtle interplay between orbital and spin contributions. We relate these surprising results to the electronic properties of the surface states of bismuth, strong Rashba spin-orbit coupling, large effective g factors, and their effect on the induced superconducting correlations.

73.63.-b, 74.45.+c, 74.78.-w, 74.78.Na

PACS numbers:

In the superconducting proximity effect, singlet pair correlations can penetrate quite far (on the micron scale) into a non superconducting (normal) conductor. This penetration, that can lead to supercurrents through normal conductors several micrometers long connected to two superconductors, results from quantum interference between all conduction channels in the sample. In a microscopic picture, the supercurrent is carried by Andreev states, combinations of time reversed electron and hole wavefunctions confined to the normal conductor. It is thus natural to consider that this interference is destroyed not only by inelastic scattering, but also by time reversal symmetry breaking. Indeed, a magnetic field is known to suppress the supercurrent via both orbital (Aharonov Bohm phase accumulation) and spin (Zeeman dephasing) effects. Nevertheless, supercurrents have been induced through ferromagnets. The oscillatory sign and decaying intensity of the supercurrent with increasing ferromagnet thickness is an illustration of the dephasing role played by the exchange field. On the other hand, the time reversal invariant spin orbit interactions, by imposing strong correlations between spatial and spin components of the induced Andreev pairs, offer new possibilities such as coupling between singlet and triplet pairing [1, 2], arbitrary Josephson phase shifts in an exchange or a Zeeman field (ϕ junction behavior) [3, 5, 6] and the possible formation of Majorana fermions at the interface between semiconducting nanowires and superconducting electrodes [4].

In this Letter, we probe the superconducting proximity effect in crystalline bismuth nanowires, a system

with extremely high Rashba spin orbit coupling (SOC), connected to superconducting electrodes with standard s-wave pairing and a very high critical field H_c . The complex interference pattern we measure, up to magnetic fields such that the Zeeman energy, E_Z , becomes of the order of the spin-orbit and Fermi energies (E_F), uniquely reveals the role played by both spin and orbital degrees of freedom.

Bismuth is a semi-metal with rhombohedral structure whose bulk electronic properties have been extensively studied: three barely filled electron bands coexist with a single, nearly filled, heavy hole band. Bi's strong atomic spin orbit energy leads to extremely high effective g factors ($g_{eff} \sim 100$), that depend on the applied magnetic field direction. Moreover the semi-metallic character leads to unusually large Fermi wavelengths, $\lambda_F \sim 50$ nm [7]. Therefore in nanostructures only a few λ_F thick or wide, because of quantum confinement, the surface states rather than the bulk states should play a major role, in particular in the transport properties [8, 9]. Angle-resolved photoemission (ARPES) revealed electronic surface states in Bi with almost free electronic mass and nanometer-size λ_F . These states are remarkable in that the energy bands display a huge Rashba spin splitting, because of the loss of inversion symmetry at the surface combined with Bi's high atomic SOC. ARPES of differently oriented Bi surfaces [10] and spin resolved ARPES [11] have found spin splitting energies of about 0.1 eV, as high as E_F . The (111) surface, perpendicular to the rhombohedral axis, is particular because it

possesses states on the top bilayer, that are decoupled from the bulk states. One dimensional quantum spin Hall states have even been predicted at the edge of these (111) surfaces [15]. Quite recently, scanning tunneling microscopy have indeed found 1D edge states around single crystalline bilayer islands on the top of BiSe or bulk Bi(111) crystals [12, 13]. 1D topological states of (114) surfaces have also been seen by ARPES [14]. Thus 100 nm-wide Bi nanowires seem ideal to investigate the effect of SOC on the superconducting proximity effect, in a regime barely explored up to now, in which the spin-splitting energy of carriers is comparable to E_F . In addition, the surface states' relatively high g_{eff} (between 10 and 100, depending on the surface orientation with respect to the magnetic field) [16], imply that E_Z can also reach E_F and spin splitting energy at fields on the 10 T scale. Finally, the relative directions between the Zeeman and orbital fields can be varied, leading to even richer physics.

In the following, we present experiments on Bi nanowires connected to high H_c superconducting electrodes that show striking differences with ordinary Josephson SNS junctions: the supercurrent persists up to magnetic fields as high as the H_c of the electrodes (11 T). In some cases the field even enhances the critical current I_c . In addition, we find oscillations of I_c : some samples display both a periodic squid-like oscillation with a period in the hundred Gauss range and a higher, Tesla range, modulation, while in other samples only a strong high field modulation is found, with the complete extinction of I_c at specific fields. These findings point to the existence of interfering Andreev pairs confined to a small number of conducting regions of low dimensionality. A subtle interplay between orbital and spin contributions is also required to explain the extent and period of interference. We discuss these unusual results in view of the properties of Bi's surface states, the very strong Rashba SOC, and high anisotropic g_{eff} .

The Bi nanowires are electrochemically grown in the 90 ± 10 nm-wide pores of a polycarbonate track-etched membrane, and released by dissolution of the membrane (supplementary materials). X-ray diffraction and transmission electron microscopy demonstrate the high crystallinity of the few- μm -long nanowires, with no high angle grain boundaries. An approximately 10 to 20 nm-thick external amorphous layer is also found, probably a protective residual polycarbonate coating. Given the nm-size λ_F of Bi's surface states [7], more than 100 conduction channels are expected at the surface of the wires. The nanowires are most likely faceted polyhedra, with each facet having a potentially different crystalline orientation. Thus some facets can be insulating [20] while others, such as (111) or (114) facets, may have very specific conduction properties. The nanowires are deposited onto an oxidized Si substrate with prepatterned electrodes. The superconducting contacts to the Bi nanowires, and

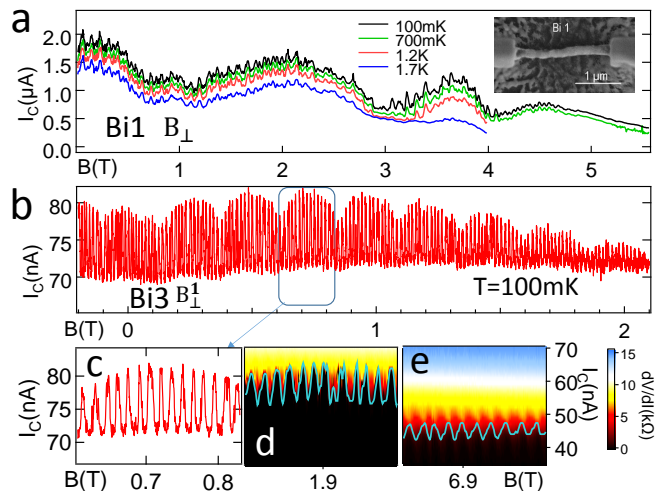


FIG. 1: Magnetic field dependence of the supercurrent of Bi_1 (a) and Bi_3 (b-e), in a perpendicular field. Fast, squid-like oscillations with periods of 800 and 150 G for Bi_1 and Bi_3 respectively, are noticeable, up to unusually high fields (at least 6 T for Bi_1 , 10 T for Bi_3). Bi_3 displays an additional periodic modulation with a 2300 G period, and an irregular modulation of Bi_1 's critical current occurs on the Tesla scale. Two kinds of switching measurements were performed on Bi_3 , with different time scales. As expected, the faster measurements (b) and (c) yield somewhat higher switching currents than the slow measurements (d) and (e). Inset: Scanning electron micrograph of Bi_1 and its superconducting contacts.

connection to the electrodes, are realized in a dual electron and ion beam microscope equipped with a gas injection system: the focused Ga ion beam (FIB) decomposes a tungsten carbonyl vapor, producing a carbon and gallium-doped amorphous tungsten wire roughly 100 nm thick and wide. The superconductive properties of these wires are impressive, with a transition temperature $T_c \sim 4$ K, $I_c \sim 100$ μA , and H_c above 11 T at low temperature (LT) [18]. The superconducting gap measured by scanning tunneling spectroscopy [19] is $\Delta = 0.8$ meV. We have checked that SNS junctions with μm -long Au wires contacted in this way behave similarly to more conventionally fabricated SNS junctions [22]. Because the FIB can be used to etch the Bi wire and coating at the contact before W deposition, this technique ensures a good, albeit not perfect, transparency. The contacts degrade with time, so the samples were cooled within hours of their connection, except for one sample (Bi_3 , see below) that was kept several weeks in vacuum at 300K after the first set of measurements, and whose resistance doubled.

We have investigated the LT resistance of ten such samples. Below the T_c of the W electrodes, the resistance is mostly due to the two probe resistance of the Bi nanowires. Although the wires have similar dimensions, this resistance varies widely, between 1 and 30 k Ω . Since the intrinsic resistance of the Bi wires is only expected to

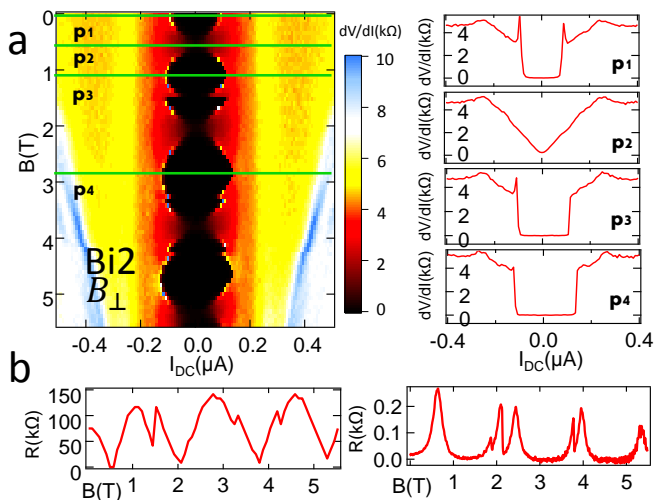


FIG. 2: (a) Color-coded differential resistance of Bi_2 , as a function of dc current and magnetic field, with some characteristic differential resistance curves on the right. (b) and (c) Field dependence of I_c and zero bias differential resistance extracted from (a). Note the oscillatory behavior on the Tesla scale, and also how the maximal critical current increases with field.

be few hundred Ω (if one extrapolates reports on much longer wires of similar diameters [8]), this indicates that the wire/contact interface resistance dominates.

Proximity induced superconductivity gives rise to a resistance decrease below the T_c of the W electrodes in five samples out of ten. A supercurrent, corresponding to a zero resistance state, is detectable in three samples. Two other samples display an incomplete proximity effect: the resistance drop is small (3 to 10 percent), and turns into a resistance increase (of about 10 percent) as the temperature is lowered further. The LT differential resistance of those two samples is peaked at low current, due to the interplay of interactions and a low transparency of the Bi/W interface [25]. These results are an indication that our Bi nanowires are not *intrinsically* superconducting, in contrast to the superconductivity below 1 K found in prior work on Bi nanowires [24]. Those nanowires were unprotected against oxidation, resulting in more pronounced surface disorder than ours. Kobayashi et al. also found intrinsic superconductivity with $T_c = 8$ K and $H_c = 4$ T in highly disordered nanowires with nm-size grains, but no intrinsic superconductivity down to 0.5 K in oxide-free crystalline Bi nanowires [26]. There is however one report of intrinsic superconductivity in arrays of single crystal Bi nanowires grown, as ours, in polycarbonate membranes (but with a different electrolyte) [17], with $T_c \sim 0.64$ K and H_c smaller than 0.5 T.

In the following we focus on the 3 samples with a detectable supercurrent, Bi_1 , Bi_2 and Bi_3 , all of which are $2\mu\text{m}$ long. Their normal state resistances R_N , measured below the W wires' T_c , are respectively 1, 13 and

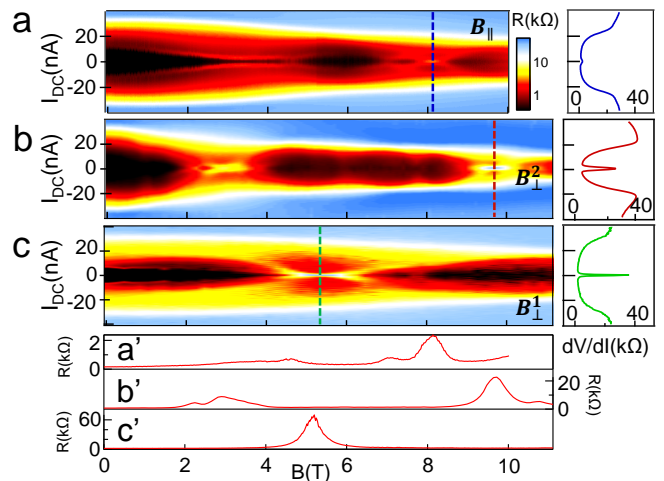


FIG. 3: Color-coded differential resistance as a function of current and field, and extracted curves, for 3 field orientations, on sample Bi_3^* (that corresponds to sample Bi_3 after thermal cycling and aging). (a) field along the nanowire axis; (b), (c) two field orientations perpendicular to the wire axis.

16 k Ω . We also present successive cool downs of Bi_3 , with changed orientations between wire and field. The sample is called Bi_3^* since its room temperature resistance increased to 27 k Ω , implying a worsening of the contact to the W electrodes. The zero bias resistance drops to zero below 0.8 K, and the differential resistance curves display a zero resistance state for currents below a switching current of 1.5, 0.1, and 0.075 μA for Bi_1 , Bi_2 and Bi_3 respectively, in zero magnetic field and at 100 mK. In the following, we equate this switching current and I_c . We also extrapolate $I_c = 30\text{nA}$ for Bi_3^* even though it does not display a fully zero resistance state. The $R_N I_c$ product ranges between 0.75 and 1.5 meV, the same order of magnitude as the superconducting gap of the W wires. This is consistent with what is expected of short Josephson SNS junctions with an induced gap of the order of the gap of the electrodes. The short junction behavior implies that the superconducting gap is less than 10 times the Thouless energy $\hbar D/L^2 \sim \hbar v_F l_e/L^2$ [23]. A Fermi velocity $v_F \leq 3 \cdot 10^5$ m/s yields a mean free path $l_e \simeq 2\mu\text{m} \simeq L$, which confirms the ballistic nature of transport through the wires. The temperature dependence of Bi_3 's differential resistance, and the Shapiro steps under irradiation at frequency f , that appear at the expected dc voltages $2eV_n = nhf$, are shown in supplementary materials.

Our most striking result concerns the magnetic field dependence of I_c (see Figs. 1 and 2, with the field perpendicular to the wires, and Fig. 3 with 3 different orientations). First, we find that the supercurrent persists up to very high fields: higher than 6 T for Bi_1 and Bi_2 , and 11 T for Bi_3 : in all cases those values are merely limited by the highest field achievable with the superconducting

magnets used in the experiments. Second, I_c of all three samples is strongly modulated by the magnetic field: two samples, Bi_1 and Bi_3 , display SQUID-like oscillations of I_c , with a period of 800 G for Bi_1 and 140 G for Bi_3 . These rapid oscillations persist to high fields, up to 10 T for Bi_3 (not shown).

The critical current of Bi_3 is also modulated with a second period of about 0.3 T. Finally, I_c is also modulated aperiodically on the Tesla scale for Bi_1 , Bi_2 and Bi_3^* (see Figs. 1, 2 and 3). In samples without rapid SQUID-like oscillations, the high field modulation causes a full extinction of the supercurrent in Bi_2 and Bi_3^* , with entire magnetic field intervals having zero supercurrent and finite resistance. We also explored 3 perpendicular field orientations for Bi_3^* , including one along the wire axis (Fig. 3). The field modulation patterns of I_c differ. High resistance peaks occur at different fields (8, 9 and 5 T, see Fig. 3). The small-period, squid-like oscillations of the first cool-down are not detectable in these subsequent cool downs.

We now discuss these complex interference patterns by considering field-induced phase shifts of the Andreev pairs wave functions, whose origin, involve either orbital or spin degrees of freedom. We first recall the generic field dependence of I_c of ordinary SNS junctions, with a very high number of conduction channels. I_c is strongly suppressed by magnetic field due to two different pair breaking mechanisms. In the semi-classical limit (λ_F much smaller than all sample dimensions), orbital phase breaking is due to the Aharonov Bohm phase difference between different Andreev pairs that follow different trajectories through the N. This orbital dephasing suppresses the supercurrent at fields corresponding to a flux quantum through the sample, as observed experimentally e.g. in Au wires [22]. In samples with a very small area perpendicular to the magnetic field, this orbital dephasing is weak, and the spin phase breaking caused by the Zeeman effect becomes noticeable. The Zeeman effect causes a phase difference between the electron and hole components of a given Andreev pair, given by $E_Z\tau/\hbar$ on a trajectory of length L_t ($\tau = L_t/v_F$ is the time to cross the sample). Summing the contributions of all Andreev pairs trajectories, when the number of channels is large, yields an exponential supercurrent suppression with magnetic field.

All three Bi wires have an area perpendicular to the magnetic field of $2 \mu m$ by $100 nm$, so that one flux quantum corresponds to a magnetic field of 50 G, three orders of magnitude smaller than the supercurrent extinction field found in the experiment. The persistence of supercurrents to fields as high as 10 T can only be understood if transport is confined to very few, quasi ballistic, 1D channels whose width should not exceed λ_F . These channels could be located along the edges of particular facets parallel to the nanowire axis [28]. The small period (few 100 G), SQUID-like oscillations of I_c in Bi_1 and Bi_3 , are

then the manifestation of quantum interference between Andreev pairs belonging to two such 1D edge channels. Such topological edge states could be those of the (111) or (114) surfaces, or of others possessing similar topological properties. Since the period of the oscillation corresponds to the flux enclosed between the interfering channels, the measured periods of 140 G for Bi_3 and 800 G for Bi_1 would correspond to 1D channels along the samples axis, distant by 70 and 12 nm respectively. This interference pattern, that we interpret as due to the concentration of current along certain edges, recalls the recent observation of periodic oscillations of the Josephson current carried by spin Hall edge states in a 2D topological insulator connected to superconducting electrodes [27].

We now discuss the supercurrent modulations at higher field, and argue that they are due to the difference between the electron and hole wavevectors of the Andreev pairs. The magnetic field, via E_Z , shifts the wavevectors of carriers of opposite spin at the Fermi level [5, 6]. Within linear approximation, the phase difference accumulated between the electron and hole components of opposite spin along a 1D ballistic trajectory of length L is [3, 29] $\delta\phi(B) = E_Z.L/(\hbar.v_F) = g_{eff}.\mu_B.B_{//}/(\hbar.v_F/L)$, with $B_{//}$ the field component along the spin orbit field. (Note the exact similarity to 1D ballistic superconducting/ferromagnetic/superconducting (SFS) junctions, [31]). Typical Bi surface states parameters ($v_F \simeq 3 \cdot 10^5 m/s$ and $g_{eff} = 30$) yield a characteristic modulation period in the Tesla range, so that we believe that the large field modulations of I_c seen on all the samples are due to this spin dephasing effect. The difference in actual interference pattern of the various samples, as well as for the three field orientations of Bi_3^* , is expected, given the anisotropy of the Bi facets and the corresponding different g_{eff} , that can vary by more than an order of magnitude. It is easy to reproduce the experimental data on Bi_3 by considering the interference between two channels of transmissions differing by a factor 8, enclosing a surface of the order of the sample area. One has to take $g_{eff} \sim 100$ for the weakly transmitting channel, yielding an amplitude modulation of the small-period orbital SQUID-like oscillations with a 0.3 T period, and a much smaller g_{eff} for the strongly transmitting channel [30].

In this picture, the full extinction of the supercurrent at nearly periodic field values is attributed to the Zeeman-induced $(2n + 1)\pi$ phase differences (with n integer) between the electron and hole components of the supercurrent-carrying Andreev pairs. Such full extinction (complete destructive interference) is thus restricted to a single current-carrying channel. This seems to be the case in Bi_2 and Bi_3^* , since they do not display SQUID-like oscillations (that require two channels). The Bi_3^* behavior is especially dramatic around 5 T (Fig. 3 c and c'), with a zero bias resistance that peaks at a value even higher than the normal state resistance. A final impor-

tant finding is the enhancement of I_c by the magnetic field. Bi_2 's critical current at 5 T is twice that of zero field (Fig. 2a and b). A similar but smaller increase between 0 and 0.75 T is also seen in Bi_3 (Fig. 1b). This increase of I_c with field may be attributable to the strong SOC, as predicted in ϕ junctions [3, 30].

We have shown evidence of quantum interference in Bi nanowires-based Josephson junctions, that persist up to very high magnetic fields. Sample dependent periodic oscillations of the critical current reveal complex interference patterns involving both orbital and spin degrees of freedom between a small number of strongly confined 1D channels, possibly located at the edges between facets of different crystalline orientations along the wires. The physical origin of this confinement of induced superconductivity in such quasi one-dimensional channels is not yet well understood. One possibility is that the confinement is favored in the superconducting state by the high magnetic field, that is known to induce inhomogeneous superconductivity in 2D superconductors with large Rashba SOC [32].

We acknowledge fruitful discussions with Alexei Chelianskii, Michael Feigelman, Pavel Ioselevich, Pascal Simon, Sacha Buzdin and Sergey Mironov. This work is supported by a Franco-Russian RFBR grant 13-02-91058-CNRS. The LPS group benefits from financial support from CNRS and of the French national research agency (ANR SUPERGRAPH and MASH).

-
- [1] Lev P. Gor'kov and Emmanuel I. Rashba, Phys. Rev. Lett. **87**, 037004 (2001).
- [2] F. S. Bergeret, A. F. Volkov, K. B. Efetov Rev. Mod. Phys. **77**, 1321 (2005).
- [3] A. Buzdin, Phys. Rev. Lett. **101**, 107005 (2008).
- [4] R. M. Lutchyn, J. D. Sau, and S. D. Sarma, Phys. Rev. Lett. **105**, 077001 (2010). V. Mourik , K. Zuo, S. M. Frolov, S. R. Plissard, E. P. A. M. Bak and L. P. Kouwenhoven, Science **336** 1003 (2012).
- [5] A. A. Reynoso G. Usaj, C. A. Balseiro, D. Feinberg, and M. Avignon, Phys. Rev. B **86**, 214519 (2012).
- [6] Tomohiro Yokoyama, Mikio Eto, Yuli V. Nazarov Phys. Rev. B **89**, 195407 (2014.)
- [7] P. Hoffman, Progress in Surface Science **81** 191245 (2006).
- [8] A. Nikolaeva , D. Gitsu, L. Konopko, M. J. Graf, and T. E. Huber Phys. Rev. B **77**, 075332 (2008).
- [9] Wei Ning *et al.* arXiv:1404.5702
- [10] Yu. M. Koroteev G. Bihlmayer, J. E. Gayone, E. V. Chulkov, S. Bl'igel, P. M. Echenique, and Ph. Hofmann Phys. Rev. Lett. **93**, 046403(2004).
- [11] Hirahara *et al.* Phys. Rev. B **76**, 153305 (2007).
- [12] Fang Yang, Lin Miao, Z. F. Wang, Meng-Yu Yao, Fengfeng Zhu, Y. R. Song, Mei-Xiao Wang, Jin-Peng Xu, Alexei V. Fedorov, Z. Sun, G. B. Zhang, Canhua Liu, Feng Liu, Dong Qian, C. L. Gao, and Jin-Feng Jia Phys. Rev. Lett. **109**, 016801 (2012).
- [13] Ilya K. Drozdov, A. Alexandradinata, Sangjun Jeon, Stevan Nadj-Perge, Huiwen Ji, R. J. Cava, B. A. Bernevig, Ali Yazdani arXiv:1404.2598
- [14] J. W. Wells , J. H. Dil, F. Meier, J. Lobo-Checa, V. N. Petrov, J. Osterwalder, M. M. Ugeda, I. Fernandez-Torrente, J. I. Pascual, E. D. L. Rienks, M. F. Jensen, and Ph. Hofmann Phys. Rev. Lett. **102**, 096802 (2009)
- [15] S. Murakami, Phys. Rev. Lett. **97**, 236805 (2006).
- [16] Babak Seradjeh, Jiansheng Wu, and Philip Phillips, Phys. Rev. Lett. **103**, 136803 (2009).
- [17] Zuxin Ye, Hong Zhang, Haidong Liu, Wenhao Wu and Zhiping Luo, Nanotechnology **19**, 085709, (2008).
- [18] A.Yu. Kasumov , K. Tsukagoshi, M. Kawamura, T. Kobayashi, Y. Aoyagi, K. Senba, T. Kodama, H. Nishikawa, I. Ikemoto, K. Kikuchi, V.T. Volkov, Yu.A. Kasumov, R. Deblock, S. Gueron, and H. Bouchiat Phys. Rev. B **72**, 033414 (2005).
- [19] Guillamon, I. *et al.* New J. Phys. **10**, 093005, (2008).
- [20] M. Wada, S. Murakami, F. Freimuth and G. Bihlmayer, Phys. Rev. B **83**, 121310 (2011).
- [21] A. A. Golubov, M. Yu. Kupriyanov, and E. Ilichev, Rev. Mod. Phys. **76**, 411 (2004).
- [22] F. Chiodi , M. Ferrier, S. Guéron, J. C. Cuevas, G. Montambaux, F. Fortuna, A. Kasumov, H. Bouchiat Phys. Rev. B **86**, 064510 (2012).
- [23] P. Dubos , H. Courtois, B. Pannetier, F. K. Wilhelm, A. D. Zaikin, and G. Sch'on Phys. Rev. B **63**, 064502 (2001).
- [24] Mingliang Tian , Jian Wang, Qi Zhang, Nitesh Kumar, Thomas E. Mallouk, and Moses H. W. Chan, Nano Lett. **9**, 3196 (2009).
- [25] H.T. Man, T.M. Klapwijk and A.F. Morpurgo arXiv:cond-mat/0504566v1
- [26] Mingliang Tian , Jinguo Wang ,Nitesh Kumar , Tianheng Han , Yoji Kobayashi , Ying Liu , Thomas E. Mallouk , and Moses H. W. Chan Nano Lett. **6** 2773, (2006).
- [27] Sean Hart , Hechen Ren, Timo Wagner, Philipp Leubner, Mathias Mhlbauer, Christoph Brne, Hartmut Buhmann, Laurens W. Molenkamp, Amir Yacoby arXiv:1312.2559 arXiv:1403.2747
- [28] An alternative hypothesis could be that the nanowires behave as nearly perfect ballistic cylinders, with a quasi-full cancellation of the flux of a perpendicular magnetic field. But we doubt this ideal picture can realistically describe our samples, see [29].
- [29] P. Ioselevich, M. Feigelman (unpublished).
- [30] S. Mironov, A. Buzdin (unpublished).
- [31] A. I. Buzdin Rev. Mod. Phys. **77**, 935 (2005).
- [32] V. Barzykin and L. P. Gorkov, Phys. Rev. Lett. **89**, 227002 (2002), O. V. Dimitrova and M. V. Feigelman, JETP Letters **78**, 637 (2003).